

Efavirenz primary and secondary metabolism *in vitro* and *in vivo*: identification of novel metabolic pathways and cytochrome P450 (CYP) 2A6 as the principal catalyst of efavirenz 7-hydroxylation.

Evan T. Ogburn, David R. Jones, Andrea R. Masters, Cong Xu, Yingying Guo, Zeruesenay

Desta

Indiana University School of Medicine, Indianapolis, IN, (ETO, DRJ, ARM, CX, ZD)

Drug Disposition Labs and Business Operations Lilly Research Laboratories, Indianapolis, IN
(YG)

Running Title Page

a) Running title: Novel metabolic pathways of efavirenz and role of CYP2A6.

b) Correspondence:

Zeruesenay Desta, PhD

Associate Professor of Medicine, Pharmacology and Toxicology

Department of Medicine/Division of Clinical Pharmacology

Indiana University School of Medicine

1001 West 10th Street, WD Myers Bldg., W7123 Indianapolis, IN 46202, USA

E-mail: zdesta@iupui.edu;

Telephone: (317) 630 8860;

Fax: (317) 630 8185

c) Number of:

text pages: 26

tables: 3

figures: 9

references: 40

words in Abstract: 231

words in Introduction: 744

words in Discussion: 1474

d) Abbreviations:

CYP, Cytochrome P450; HPLC, high performance liquid chromatography; MS, mass

spectrometry; MRM, Multiple Reaction Monitoring; HLM, human liver microsome; K_m ,

Michaelis-Menten constant; V_{max} , maximum enzyme velocity; IC_{50} , half maximal inhibitory

concentration, EFV, Efavirenz; 7- and 8-OHEFV, 7- and 8-hydroxyefavirenz; 8,14-diOHEFV,

8,14-dihydroxyefavirenz; diOHEFV, dihydroxylated efavirenz;

ABSTRACT

Efavirenz primary and secondary metabolism was investigated *in vitro* and *in vivo*. In human liver microsome (HLM) samples, 7- and 8-hydroxyefavirenz accounted for 22.5% and 77.5% of the overall efavirenz metabolism, respectively. Kinetic, inhibition and correlation analyses in HLM samples and experiments in expressed cytochrome P450 (CYP) show that CYP2A6 is the principal catalyst of efavirenz 7-hydroxylation. While CYP2B6 was the main enzyme catalyzing efavirenz 8-hydroxylation, CYP2A6 also seems to contribute. 7- and 8-hydroxyefavirenz were further oxidized to novel dihydroxylated metabolite(s) primarily by CYP2B6. These dihydroxylated metabolite(s) were not the same as 8,14-dihydroxyefavirenz, a metabolite that has been suggested to be directly formed via 14-hydroxylation of 8-hydroxyefavirenz, because 8,14-dihydroxyefavirenz was not detected *in vitro* when efavirenz, 7-, or 8-hydroxyefavirenz were used as substrates. Efavirenz and its primary and secondary metabolites that were identified *in vitro* were quantified in plasma samples obtained from subjects taking a single 600 mg oral dose of efavirenz. 8,14-Dihydroxyefavirenz was detected and quantified in these plasma samples, suggesting that the glucuronide or the sulfate of 8-hydroxyefavirenz might undergo 14-hydroxylation *in vivo*. In conclusion, efavirenz metabolism is complex involving unique and novel secondary metabolism. While efavirenz 8-hydroxylation by CYP2B6 remains the major clearance mechanism of efavirenz, CYP2A6-mediated 7-hydroxylation (and to some extent 8-hydroxylation) may also contribute. Efavirenz may be a valuable dual phenotyping tool to study CYP2B6 and CYP2A6, and this should be further tested *in vivo*.

INTRODUCTION

Efavirenz-based antiretroviral therapy continues to be the preferred initial therapy in the treatment of naïve HIV-1/AIDS patients, but its use is associated with variable treatment response and adverse effects in most part due to the large differences in pharmacokinetics (Marzolini et al., 2001; Csajka et al., 2003). Efavirenz is predominantly cleared by hepatic metabolism (Mutlib et al., 1999b). The metabolites identified in human plasma and urine (almost exclusively as glucuronide or sulfate conjugates) were 7- and 8-hydroxyefavirenz (primary metabolites) and 8,14-dihydroxyefavirenz (secondary metabolite). Thus, factors that alter efavirenz clearance could influence efficacy or toxicity of the drug.

Cytochrome P450 (CYP) 2B6 is the main enzyme catalyzing the major clearance mechanism of efavirenz, 8-hydroxylation to 8-hydroxyefavirenz, *in vitro* (Ward et al., 2003; Desta et al., 2007). Clinical studies in HIV patients have repeatedly shown that CYP2B6 genetic variants with functional consequences are associated with higher efavirenz exposure and in some studies with increased risk for adverse CNS effects compared to those without variants (Zanger et al., 2007). However, not all efavirenz pharmacokinetic variability could be explained by the 8-hydroxylation pathway or CYP2B6 alone as a large intersubject variability in efavirenz exposure remains even after accounting for known CYP2B6 genetic variations (Rotger et al., 2007; Arab-Alameddine et al., 2009). Other CYPs that include expressed CYP3A4/5 and CYP1A2 show activity towards efavirenz 8-hydroxylation *in vitro* (Ward et al., 2003), but the *in vivo* contribution of these enzymes, if any, appears to be marginal (Mouly et al., 2002; Tsuchiya et al., 2004; Bristol-Myers Squibb Company 2009). Metabolic pathways other than efavirenz 8-hydroxylation may also contribute to efavirenz clearance. Efavirenz 7-hydroxylation to 7-hydroxyefavirenz has been demonstrate *in vitro* (Ward et al., 2003; Desta et al., 2007) and *in*

in vivo animal and human studies (Mutlib et al., 1999b), although the contribution of this route to the overall clearance of efavirenz and the enzymes involved remains poorly defined. Correlation analysis between the activity of CYP enzymes and formation rates of 7-hydroxyefavirenz in a small panel of HLMs (Ward et al., 2003) implicated CYP2A6 compared to other CYPs ($r=0.45$; $p=0.19$). A significant correlation between formation rate of 7-hydroxyefavirenz and CYP2A6 protein (Spearman $r=0.395$, $p<0.0001$) and activity ($r=0.583$, $p<0.0001$) was observed in a subsequent study involving a large panel of human liver samples (Desta et al., 2007). However, it was difficult to ascertain the contribution of this enzyme in efavirenz 7-hydroxylation as a significant correlation between CYP2A6 protein and activity with CYP2B6 protein and activity as well as formation rate of 8-hydroxyefavirenz was also observed (Desta et al., 2007). Recent association studies in HIV patients support the role CYP2A6 may play in efavirenz clearance (Kwara et al., 2009a, 2009b; di Iulio et al., 2009; Arab-Alameddine et al., 2009). However, direct evidence linking CYP2A6 or any other enzyme in efavirenz metabolism is lacking.

On the basis of largely *in vitro* studies, CYP2B6, which shows highly variable expression and activity among individuals in part due to genetic variation and exposure to inhibitors or inducers, metabolizes a growing list of clinically important drugs, environmental chemicals and endogenous compounds [for reviews, see: (Ekins and Wrighton 1999; Hodgson and Rose 2007; Zanger et al., 2007; Wang and Tompkins 2008; Mo et al., 2009)]. However, information on the clinical relevance of this enzyme has been generally limited due to the lack of suitable *in vivo* substrate probe. Bupropion 4-hydroxylation has been increasingly used as *in vitro* and *in vivo* probe of activity, but its *in vivo* utility has important limitations (Kharash et al., 2008). Efavirenz has been proposed to be an alternative probe of CYP2B6 activity to evaluate the clinical relevance of this enzyme (Ward et al., 2003; US Food and Drug Administrations, 2006). To

identify and select appropriate markers (e.g. metabolic ratios) that can best describe CYP2B6 activity *in vivo*, a comprehensive characterization of the primary and secondary metabolism of efavirenz and the specific enzymes involved is important.

The main aims of this study were to use human liver cellular fractions, expressed CYPs and clinical samples collected from efavirenz treated subjects to: a) assess the contribution of efavirenz 7-hydroxylation in efavirenz elimination and to identify the specific CYP enzyme(s) catalyzing this reaction; b) characterize the metabolism of efavirenz via the 8-hydroxylation pathway to further confirm previous findings and use this as a positive control; and c) characterize more closely efavirenz secondary metabolism and identify the CYPs involved.

MATERIALS AND METHODS

Chemicals: Efavirenz, 8-hydroxyefavirenz, 7-hydroxyefavirenz, 8,14-dihydroxyefavirenz and nevirapine were obtained from Toronto Research Chemicals Inc. (Toronto, Canada). Diethyldithiocarbamate, ketoconazole, furafylline, omeprazole, pilocarpine, quercetin, quinidine, thioTEPA, ticlopidine, troleandomycin, glucose 6-phosphate, glucose-6-phosphate dehydrogenase, and NADP⁺ were purchased from Sigma-Aldrich (St. Louis, MO). Letrozole was purchased from U.S. Pharmacopeia (Rockville, MD). Sulfaphenazole was obtained from Ultrafine Chemicals (Manchester, UK). 8-Hydroxyefavirenz glucuronide was a generous gift of Dr. David Christ (DuPont Pharmaceuticals, Wilmington, DE). All other chemicals were of HPLC grade.

Microsomal preparations: Human liver microsome (HLM) samples were prepared from human liver tissues that were medically unsuitable for transplantation as described elsewhere (Jeong, et al., 2009a) or characterized HLM samples were purchased from Cellz Direct (Austin, TX) and BD Biosciences (San Jose, CA). Baculovirus-insect cell-expressed human CYPs (1A2, 2A6, 2B6, 2C8, 2C9, 2C19, 2D6, 2E1, 3A4, and 3A5) (with oxidoreductase) were purchased from BD Biosciences. HLM samples and CYPs were stored at -80°C until used.

LC/MS/MS assay method: A new selective and sensitive LC/MS/MS method was developed to detect and quantify efavirenz and its known metabolites in microsomal incubates because a previously used HPLC method (Ward, et al., 2003) lacked sensitivity to quantify metabolites produced at low rate. The MS/MS system was an API 2000 MS/MS triple quadrupole system (Applied Biosystems, Foster City, CA) equipped with a turbo ion spray and was coupled with a Shimadzu HPLC system consisting of a LC-20AB pump and SIL-20A HT autosampler (Shimadzu Addison, IL), all controlled by AnalystTM 1.4.2 software (Applied Biosystems/MDS

Sciex) in conjunction with Windows 2000. Separation of compounds was achieved using a reverse phase chromatography using a Phenomenex Luna C₁₈ column (100 x 2 mm, 3 μm) (Phenomenex, Torrance, CA) and a mobile phase that consisted of acetonitrile and 0.1% formic acid (50:50; v/v) (isocratic flow rate 0.15 mL/min).

Stock solutions of efavirenz, 7-hydroxyefavirenz, 8-hydroxyefavirenz, 8, 14-dihydroxyefavirenz, and nevirapine (internal standard) were prepared separately in polypropylene tubes by adding methanol to a concentration of 1 mg/mL. These stock solutions were stored at -20°C. Serial dilutions were performed from the stock solutions in methanol and mobile phase for MS/MS optimization experiments. Parent and fragment ions were detected in multiple-reaction monitoring (MRM) mode. All of the analytes (nevirapine, efavirenz, 7- and 8-hydroxyefavirenz, and 8,14-dihydroxyefavirenz) were observed under unit resolution for quadrupoles 1 and 3. Mass spectrometry optimization was performed by adjustments of the source- and the compound-dependent parameters as listed in supplemental Table 1. Optimal gas pressures for all of the analytes were: nitrogen nebulizer gas 10 psi, curtain gas 10 psi, collision gas 3.0 psi, ion source gas (1) 24 psi, source gas (2) 41 psi. Other parameter settings were: ion spray voltage: -4500 V in negative mode (4200 V in positive mode); and source temperature of 470°C. Efavirenz and its metabolites were measured with the quantifier MRM and confirmed with the qualifier MRM transition (Supplemental Table 1). The MRM scan was performed in positive ion mode for the internal standard (nevirapine) and in negative ion mode for efavirenz and its metabolites. The quantifier and qualifier transitions were selected based on the signal intensity of the metabolite peaks (Supplemental Table 1). The parent and daughter ions were the same for 7- and 8-hydroxyefavirenz. Therefore, the two metabolites were quantified after chromatographic separation.

Identification/confirmation of efavirenz metabolites: Pilot incubation experiments were performed as described previously with slight modification (Ward et al., 2003; Desta, et al., 2007) to identify potentially new metabolites and/or confirm the presence of known efavirenz primary and secondary metabolites. Efavirenz was used as a substrate to determine primary metabolites, whereas 7- and 8-hydroxyefavirenz as well as 8-hydroxyefavirenz glucuronide were used as substrates to assess secondary metabolism. Substrates (in methanol) were added to a tube and solvent was evaporated. Residue was reconstituted with phosphate reaction buffer (0.2M Na₂HPO₄ titrated with 0.2M NaH₂PO₄ to a pH of 7.4) and a mixture of efavirenz (20 μM) [or 7- or 8-hydroxyefavirenz, 5 μM; 8-hydroxyefavirenz glucuronide, 50 μM] and HLMs (1 mg/ml) was allowed to equilibrate for 5 min at 37°C (final volume, 250 μl). The reaction was initiated by adding a NADPH-generating system (cofactors) (13 mM NADP, 33 mM glucose 6-phosphate, 33 mM MgCl₂, and 0.4 U/mL glucose 6-phosphate dehydrogenase) and allowed to proceed for 30 min at 37°C. After terminating the reaction by immediately adding 500 μl of acetonitrile and placing tubes on ice, nevirapine (20 μL of 5 μg/ml) was added as an internal standard for the incubation sample of efavirenz and 7- and 8-hydroxyefavirenz. Ritonavir (25 μl of 0.01mg/mL) was used as an internal standard for incubation consisting of 8-hydroxyefavirenz glucuronide. All samples were vortex mixed for 30 seconds, and centrifuged at high speed for 5 min in an Eppendorf model 5415D centrifuge (Brinkmann Instruments, Westbury, NY).

The supernatant was removed, transferred to another tube and extracted with ethyl acetate under alkaline pH as described previously (Ward, et al., 2003). After centrifugation for 15 minutes at 2500 rpm in a Beckman Coulter - Allegra® 6R Benchtop Centrifuge, the organic layer was removed, transferred to another tube, and evaporated to dryness. The residue was reconstituted with 50 μl of mobile phase from which 10 μl was injected onto the LC/MS/MS

system described below (efavirenz, and 7- and 8-hydroxyefavirenz incubations). For 8-hydroxyefavirenz glucuronide incubation, the residue was reconstituted in 150 μ l of mobile phase from which 100 μ l was injected onto HPLC-UV/Vis system (Ward, et al., 2003) that consisted of a Zorbax SB-C₁₈ column (150 x 4.6 mm, 3.5 μ m particle size; Phenomenex, Torrance, CA), a LunaC₁₈ Guard column (30 x 4.6 mm, 5 μ m; Phenomenex), and a mobile phase composed of 65% 10 mM KH₂PO₄ (adjusted to pH 2.4 with 1% phosphoric acid) and 35% (v/v) acetonitrile (flow rate, 0.8 mL/min). Negative control incubations consisting of no substrate, no cofactors, or no microsomes (bovine serum albumin was used instead) were run in parallel and processed as above.

Retention times, precursor ions (Q1) scan data obtained under negative ESI conditions ([M + H]⁺ m/z 330 for 7- and 8-hydroxyefavirenz, m/z 314 for efavirenz, and m/z 346 for 8,14-dihydroxyefavirenz) and product ion scan (Q3) spectral data of the known synthetic metabolite standards were compared with those metabolite peaks obtained from microsomal incubates to confirm previously reported efavirenz primary and secondary metabolites (7- and 8-hydroxyefavirenz, and 8,14-dihydroxyefavirenz). Precursor ions (Q1) scans were also conducted in both negative and positive ion modes under different MS settings to search for potentially new, structurally predicted, oxidative metabolites of efavirenz. If any potential metabolite peak was detected by Q1 scan, then sample and negative control incubations were re-injected in to the LC/MS/MS and subject to a product ion scan (Q3) range of m/z 100 to 400. For the 8-hydroxyefavirenz glucuronide incubations, the analysis was made using HPLC with UV detection as LC/MS/MS analysis did not yield useful information.

Linear conditions for metabolite formation with respect to protein and time were assessed prior to the subsequent studies. A final protein concentration of 0.25 mg/ml and 10-min

incubation represented linear conditions and were used. In addition, these incubation conditions were selected to minimize sequential metabolism while ensuring assay sensitivity. The same conditions were used for determination of efavirenz sequential metabolism.

Kinetic analyses: Rates of efavirenz metabolism to 7- and 8-hydroxyefavirenz was determined by incubating a range of efavirenz concentrations (1–150 μ M) in duplicate for 10 min at 37°C with characterized HLM samples (n=7; 0.25 mg protein/ml) and cofactors. The reaction was terminated and processed as described above.

Correlation analyses: Correlation between formation rates of efavirenz metabolism to 7- and 8-hydroxyefavirenz and the activity of specific isoforms was tested by incubating efavirenz (10 μ M) with a panel of 15 characterized HLM samples (0.25 mg/ml) and cofactors in duplicate for 10 min at 37°C. The activity of each CYP isoform in each HLM sample, determined by isoform-specific reaction markers, was as provided by the supplier (BD Bioscience, San Jose, CA; <http://www.bdbiosciences.com/ptDatabaseList.jsp>).

Inhibition analyses: Efavirenz (10 μ M) was incubated with HLMs (0.25 mg/ml) and the NADPH-generating system at 37°C for 10 min in the absence (control) and presence of the following known isoform-specific inhibitors: pilocarpine (50 μ M) and letrozole (50 μ M) for CYP2A6, quercetin (50 μ M) for CYP2C8, sulfaphenazole (25 μ M) for CYP2C9, ticlopidine (5 μ M) for CYP2C19 and CYP2B6, quinidine (1 μ M) for CYP2D6, and ketoconazole (1 μ M) for CYP3A. Inhibition by furafylline (20 μ M) for CYP1A2, thioTEPA (50 μ M) for CYP2B6, diethyldithiocarbamate (50 μ M) for CYP2E1 and troleandomycin (50 μ M) for CYP3A has been shown to be time-dependent. Therefore, a preincubation protocol was implemented in which the inhibitor was first incubated with HLM sample (0.25 mg protein/ml) and cofactors for 15 min at 37°C before the reaction was initiated by addition of the respective selective substrate probe. The

specific conditions for use of these inhibitors have been described in detail in previous publications (Newton et al., 1995; Bourrie et al., 1996; Rae et al., 2002; Ward et al., 2003; Jeong et al., 2009a; 2009b). Sample processing was as described above. The percent formation rate remaining after inhibition relative to the uninhibited controls (without inhibitors or vehicle controls) was calculated.

Additional experiments were performed to evaluate the role CYP2A6 and CYP2B6 plays in catalyzing efavirenz 7- and 8-hydroxylation and to assess the relative selectivity of pilocarpine and thioTEPA towards these enzymes. Efavirenz (10 μ M) was incubated for 10 min at 37°C with HLM samples (0.25 mg/ml) and cofactors in the absence (control) and presence of an inhibitor. A single concentration of thioTEPA (50 μ M) or pilocarpine (50 μ M), or multiple concentrations of thioTEPA (0-100 μ M) or pilocarpine (0-100 μ M) were used in these inhibition experiments.

Efavirenz primary and secondary metabolism by expressed CYP isoforms:

Efavirenz (10 and 100 μ M) was incubated with expressed CYP 1A2, 2A6, 2B6, 2C8, 2C9, 2C19, 2D6, 2E1, 3A4, or 3A5 (13-26 pmol) and cofactors (same composition as above) at 37°C for 10 min. The lower concentration of efavirenz is close to the K_m values while the higher concentration represents concentration at saturation (V_{max} in Michaelis-Menten curve). For those isoforms that showed substantial activity towards efavirenz metabolism, namely expressed CYP2A6 and CYP2B6, full kinetic analyses were performed by incubating efavirenz (1 to 150 μ M) with cofactors and expressed CYP2A6 (26 pmol) or CYP2B6 (13 pmol) for 10 min. In addition, inhibition of expressed CYP2A6 and CYP2B6 by thioTEPA and pilocarpine were tested by incubating efavirenz (10 μ M) with expressed CYP2A6 (26 pmol) or CYP2B6 (13 pmol) in the absence (control) and presence of thioTEPA (0-100 μ M) or pilocarpine (0-100 μ M). Further processing of incubate was as described above.

Efavirenz sequential metabolism by expressed CYPs was determined by incubating 7-hydroxyefavirenz (5 μ M), 8-hydroxyefavirenz (5 μ M) and 8-hydroxyefavirenz glucuronide (50 μ M) for 10 min with 13-26 pmol CYP and cofactors (30 min incubation was used for the glucuronide). The kinetics for the metabolism of 7- or 8-hydroxyefavirenz (1 to 150 μ M) was determined in expressed CYP2B6 (13 pmol). HPLC with UV detection (Ward, et al., 2003) and/or LC/MS/MS as described above were used to monitor metabolites formed.

***In vivo* studies:** To determine efavirenz metabolism and pharmacokinetics *in vivo*, efavirenz and its metabolites were measured in plasma samples obtained from healthy volunteers who participated in a clinical trial and received a single 600 mg oral dose of efavirenz. The clinical trial was approved by the Institutional Review Board (IRB) of the Indiana University School of Medicine. Eligible subjects participated in the trial after signing a written informed consent. Plasma samples were collected at baseline and 0.5 to 72 hours after efavirenz dosing.

A pilot study has shown that nearly all efavirenz metabolites exist predominantly as conjugates, consistent with *in vivo* evidence (Mutlib et al., 1999b). Therefore, plasma samples were analyzed after enzymatic hydrolysis (deconjugation by incubating overnight with β -glucuronidase). Plasma samples (200 μ L) were incubated with 2 mL of 0.2 M sodium acetate buffer (pH 5.0) and 100 μ L of 10,000 unit β -glucuronidase at 37°C for 17 hours. After adding the internal standard (20 μ L of 5 μ g/mL ritonavir), the samples were extracted with 5 mL ethyl acetate under alkaline pH (0.1M sodium carbonate buffer, pH 9.4). The organic layer was evaporated to dryness in SpeedVac. Residue was reconstituted in 100 μ L mobile phase and analyzed by the LC/MS/MS system described below.

The LC/MS/MS assay described *in vitro* was modified to measure plasma concentrations of efavirenz and its metabolites in clinical samples. Chromatographic analysis was performed

using an Agilent 1100 series HPLC (Agilent Technologies, Santa Clara, CA) and a LEAP Technologies model HTS PAL autosampler (Carrboro, NC) coupled with an Applied Biosystems API 3200 triple-quadrupole mass spectrometer (Applied Biosystems, Foster City, CA) equipped with a turbo ion spray in positive ionization mode and controlled by Analyst software Version 1.4.1 in conjunction with Windows 2000. The separation column used was the same as that described for *in vitro* studies. A gradient elution profile was used: initial mobile phase, 99% of 0.01% formic acid in water and 1% of methanol (v/v); and the secondary mobile phase consisted of 99% methanol and 1% of 0.01% formic acid in water. The secondary mobile phase was increased from 50% to 90% linearly between 0 to 16 min; the initial mobile phase conditions were resumed after 16 min and remained constant for an additional 4 min, allowing the column to equilibrate. The eluate was introduced, without splitting, at 0.800mL/min to the turbo ion source. Mass spectrometry optimization was achieved via adjustments of both the compound-dependent and compound-independent parameters for efavirenz, 8-hydroxyefavirenz, 7-hydroxyefavirenz and 8,14-dihydroxyefavirenz. The analytes were optimized at a source temperature of 400° C, under unit resolution for quadrupoles 1 and 3, and were given a dwell time of 100 msec and a settling time of 75 msec. Optimal gas pressures for all five analytes, including the internal standard, were: collision gas 6 psi, curtain gas 10 psi, ion source gas (1) 30 psi, ion source gas (2) 25 psi. The compound-independent mass spectrometer parameters, as well as, the parent and fragment ions that were used in multiple-reaction monitoring (MRM) mode for detection are listed in Supplemental Table 2. The limit of quantification of efavirenz and its metabolites in the *in vitro* and *in vivo* LC/MS/MS method was 3 ng/mL. The standard curve was linear over the range of 3 ng/ml to 10000 ng/ml. The day to day and within day coefficient of

variation was less than 21% at the lowest (5 ng/mL) and highest (5000 ng/ml) quality control concentrations used.

Data analysis: Apparent kinetic constants (V_{\max} and K_m) were estimated by fitting formation rates of metabolites versus substrate concentrations to appropriate kinetic equations by nonlinear regression analysis using GraphPad Prism version 5.00 for Windows, GraphPad Software (San Diego, CA; www.graphpad.com). *In vitro* intrinsic clearances (CL_{int}) represent V_{\max}/K_m . IC_{50} values were determined by analysis of the plot of the logarithm of the inhibitor concentration versus the percentage of activity remaining after inhibition using GraphPad. Correlation analysis was performed by a nonparametric test (Spearman's rank correlation test) using GraphPad. $p < 0.05$ was considered statistically significant. Data are presented as mean \pm S.D or as averages of duplicate experiments.

RESULTS

A. Primary metabolism of efavirenz *in vitro*. Two metabolites (Figure 1) that were consistent with monohydroxyefavirenz were positively identified as 7- and 8-hydroxyefavirenz based on comparison of their retention times, precursor ion scan data (molecular mass of 331) and MS/MS fragmentation patterns with synthetic metabolite standards.

Kinetic analyses: The kinetics for the formation of 7- and 8-hydroxyefavirenz from efavirenz was determined in several HLM samples. Representative Michaelis-Menten kinetic and Eadie-Hofstee plots in a HLM sample are depicted in Figure 2 and the kinetic parameters of 7 HLM samples are summarized in Table 1. The average K_m values for the formation of 7- and 8-hydroxyefavirenz were comparable (average: 14.7 μM versus 12.7 μM respectively). The *in vitro* intrinsic clearances, $CL_{int} (V_{max}/K_m)$, show high variability among HLMs (~35- and ~13-fold for 7- and 8-hydroxyefavirenz formation respectively) (Table 1). As there was no marked difference in K_m between the HLM samples tested, the interindividual difference in CL_{int} is largely driven from differences in V_{max} . The CL_{int} for formation of 8-hydroxyefavirenz was on average 3.2-fold higher than that for 7-hydroxyefavirenz. Assuming that sequential metabolism is minimal (present study) and that the contributions of other elimination pathways such as nonhepatic clearance (Mutlib et al., 1999b) and efavirenz N-glucuronidation (Belanger, et al., 2009) to overall elimination of efavirenz are minimal, 7- and 8-hydroxylation appears to account for 22.5% (range: 9.8-38.5%) and 77.5% (range: 61.5-90.2%) of the overall efavirenz metabolism *in vitro*, respectively. In the limited number of HLMs, CL_{int} values of 8-hydroxyefavirenz correlated significantly with CL_{int} values of 7-hydroxyefavirenz (Spearman $r = 0.86$; $p=0.024$), and this correlation appears to be mainly derived from V_{max} values ($r=0.71$, $p=0.088$) rather than K_m values ($r=0.21$; $p=0.66$).

Correlation analyses: The metabolism of efavirenz to 7- and 8-hydroxyefavirenz was tested in a panel of characterized HLM samples (n=15). Rates of formation 7- and 8-hydroxyefavirenz varied widely among the HLMs [formation rate of 7-hydroxyefavirenz: 16.9 ± 9.7 (range: 3.2 to 32.2) pmol/min/mg protein, 10-fold difference; and formation rate of 8-hydroxyefavirenz: 122.1 ± 103.6 (range: 13.7 to 419.2) pmol/min/mg protein, 31-fold difference] (Figure 3). The average formation rates (pmol/min/mg protein) of efavirenz metabolism to 8-hydroxyefavirenz at $10 \mu\text{M}$ efavirenz was 7.7-fold higher (range: 1.8- to 20.5-fold difference) than the formation rates of 7-hydroxyefavirenz. Comparing the rates of metabolite formation from efavirenz ($10 \mu\text{M}$), Efavirenz 7-hydroxylation accounts for $15.6 \pm 8.7\%$ (range: 4.7 to 35.9%) while the remaining is accounted by efavirenz 8-hydroxylation ($84.5 \pm 8.7\%$, range: 64.1 to 93.5%). These results are consistent with the CL_{int} data in Table 1.

Correlations between rates of efavirenz metabolism and the activities of CYP isoforms in the HLMs are summarized in Table 2. A highly significant correlation between formation rates of 8-hydroxyefavirenz and CYP2B6 activity and between formation rates of 7-hydroxyefavirenz and CYP2A6 was observed. The activities of certain other isoforms showed modest but significant correlation ($p < 0.05$) with formation rates of 7-hydroxyefavirenz (CYP2B6, CYP2C8 and CYP3A) and formation rates of 8-hydroxyefavirenz (CYP1A2, CYP2A6 and CYP2C8) (Table 2). Formation rates of 7- hydroxyefavirenz correlated weakly but significantly with formation rates of 8-hydroxyefavirenz (Spearman $r = 0.54$; $p = 0.038$) (Table 2), consistent with the CL_{int} data described above, which may reflect the significant correlation between CYP2A6 and CYP2B6 activity in the panel of HLMs studied ($r = 0.76$; $p = 0.0011$).

Efavirenz metabolism by a panel of expressed enzymes: To obtain qualitative information as to which isoforms might catalyze efavirenz primary metabolism, the ability of 10

expressed CYP enzymes to catalyze 7- and 8-hydroxylation of efavirenz (10 μ M and 100 μ M) was tested. The lower concentration of efavirenz is close to the K_m values while the higher concentration represents concentration at saturation (V_{max} in Michaelis-Menten curve). Efavirenz 7-hydroxylation was solely catalyzed by expressed CYP2A6 at both 10 and 100 μ M efavirenz (Figure 4A). None of the other isoforms tested showed any detectable 7-hydroxylase activity. As expected, CYP2B6 catalyzed efavirenz 8-hydroxylation at the highest rate at both concentrations (Figure 4B). Other isoforms (CYP1A2, CYP3A5, CYP2A6, CYP3A4, CYP2C19 and CYP2D6) also showed activity towards this reaction. Kinetic studies with expressed CYP2B6 and CYP2A6 revealed that CYP2B6 did not produce 7-hydroxyefavirenz at any of the concentrations tested (Table 1), confirming that this enzyme is not involved in efavirenz 7-hydroxylation, while CYP2A6 was involved in catalyzing 7- and 8-hydroxylation of efavirenz, with similar K_m but slightly higher V_{max} for 7-hydroxylation (Table 1). CL_{int} for CYP2A6-catalyzed 8-hydroxylation was lower than that of CYP2A6-catalyzed efavirenz 7-hydroxylation (by 1.5-fold) and CYP2B6-catalyzed efavirenz 8-hydroxylation (by 3.2-fold).

Inhibition of efavirenz metabolism by CYP-isoform specific inhibitors in HLM samples. As shown in Figure 5A, pilocarpine was the most potent inhibitor of efavirenz 7-hydroxylation (by 94%) followed by thioTEPA (by 50.3%), while ticlopidine increased formation of 7-hydroxyefavirenz (by 64%). In addition, formation of 7-hydroxyefavirenz was potently inhibited by letrozole (by 98.1%) (Figure 5A), consistent with a recent findings that letrozole is a relatively selective inhibitor of CYP2A6 (Jeong, et al., 2009b). As expected, thioTEPA and ticlopidine inhibited formation of 8-hydroxyefavirenz by over 70% (Figure 5B). Pilocarpine also inhibited formation of 8-hydroxyefavirenz by more than 60%, ketoconazole by 21% and letrozole by 27% (Figure 5B).

CYP-selective chemical inhibitors are often used to dissect the contribution of the corresponding CYP to drug metabolism. Thus, thioTEPA and pilocarpine have been considered selective inhibitors of CYP2B6 (Rae, et al., 2002) and CYP2A6 (Bourrie, et al., 1996), respectively. Although not specific, ticlopidine is also a potent inhibitor of CYP2B6 (Richter, et al., 2004). Additional inhibition experiments in HLM samples and expressed enzymes (CYP2A6 and CYP2B6) were performed to test whether inhibition of CYP2A6 by thioTEPA and of CYP2B6 by pilocarpine represents lack of selectivity of these inhibitors or involvement of both enzymes in the pathways studied, and to test whether ticlopidine's effect may involve activation of CYP2A6. The inhibition data are summarized in Table 3. ThioTEPA inhibited formation of 8-hydroxyefavirenz by 68% and 55% in HLMs (IC_{50} , 9.8 μ M) and expressed CYP2B6, respectively (IC_{50} 6.6 μ M); of 7-hydroxyefavirenz by 45% in HLMs (IC_{50} , 31.7 μ M) and by 83% in expressed CYP2A6; and of 8-hydroxyefavirenz by 83% in expressed CYP2A6 (IC_{50} , 6.9 μ M) (Table 3). Pilocarpine potently inhibited 7-hydroxylation of efavirenz (by over 94%) in HLM samples (IC_{50} , 2.3 μ M) and expressed CYP2A6; and of 8-hydroxylation in HLMs, expressed CYP2A6, and CYP2B6 by 67.3% (IC_{50} , 29.5 μ M), 93.8%, and 24.4% (IC_{50} , 49.2 μ M) respectively (Table 3). The potency of inhibition by pilocarpine of 8-hydroxylation in HLMs was approximately 2.8-fold higher than that observed with expressed CYP2B6 (Table 3). As shown in Table 3, ticlopidine increased formation of 7-hydroxyefavirenz (to 151%) in samples. However, when expressed CYP2A6-catalyzed 7- and 8-hydroxylation was assessed, no increase in formation of 7-hydroxyefavirenz was observed; instead, this reaction was slightly inhibited by ticlopidine (by <23%) (Table 3). No metabolite of ticlopidine that coelute with 7-hydroxyefavirenz was noted when ticlopidine was incubated alone with HLM samples and cofactors. As expected, ticlopidine potently inhibited efavirenz 8-hydroxylation (81.9% and 73%

respectively) in HLM samples and CYP2B6 (Table 3). Since ticlopidine minimally inhibited CYP2A6 in expressed enzyme, it is possible that there is a metabolic shift towards 7-hydroxylation in HLM samples.

B. Secondary (sequential) metabolism of efavirenz. The data presented in this section (section B) should be viewed as preliminary findings because the precise structural identities of the metabolites were not unequivocally established.

Metabolite identification in HLM samples. Beside the two monohydroxylated metabolites of efavirenz (7- and 8-hydroxyefavirenz), a third metabolite peak that was consistent with a dihydroxyefavirenz (molecular mass of 347 (with $[M-H]^-$ at m/z 346) was identified when efavirenz was incubated with HLMs and cofactors (but not in negative controls) (Figure 1). Since previous studies have suggested that 8-hydroxyefavirenz is 14-hydroxylated to form 8,14-dihydroxyefavirenz (Mutlib, et al., 1999b; Ward, et al., 2003), the possibility that the dihydroxylated metabolite of efavirenz might be 8,14-dihydroxyefavirenz was explored. The major fragment ions of synthetic 8, 14-dihydroxyefavirenz standard, determined by infusing a standard solution onto the MS/MS system set in the quantitative optimization mode, were 238 and 210 (Supplemental Table 1). The major MS/MS fragment ions of the metabolite peak observed in efavirenz HLM sample incubation was determined by injecting an aliquot of an efavirenz (20 μ M) incubation mixture onto the LC/MS/MS system/ using the product ion mode, the signal generated by the parent ion mass m/z 346 produced fragmentation product ions of 238 and 210, consistent with those of synthetic 8,14-dihydroxyefavirenz (Supplemental Fig. 1). When the retention times of the metabolite peak produced in efavirenz incubates was compared with that of synthetic standard of 8,14-dihydroxyefavirenz, marked difference was observed in the LC/MS/MS (Supplemental Fig. 1) [and HPLC with UV detection (data not shown)]. 8,14-

dihydroxyefavirenz. Therefore, as the secondary metabolite observed in efavirenz microsomal incubates appears to be different from 8,14-dihydroxyefavirenz, the unknown metabolite is designated as only dihydroxylated efavirenz.

To test whether this dihydroxylated metabolite was also formed from the primary metabolites of efavirenz (7- or 8-hydroxyefavirenz), each metabolite was incubated with HLM samples and cofactors. Incubation of 7- (Figure 6A) and 8-hydroxyefavirenz (Figure 6B) resulted in the appearance of a peak that coeluted chromatographically with the dihydroxylated efavirenz. This peak was not observed in the negative control experiments. Again, the precursor and product ion scans of the metabolite formed from these substrates were the same as those from synthetic 8,14-dihydroxyefavirenz standard, but the retention time (6.8 min) of the dihydroxylated efavirenz was markedly different from that of 8,14-dihydroxyefavirenz (4.66 min) (Figure 6C).

Secondary metabolism in expressed CYPs. To identify the CYP isoforms involved in efavirenz sequential metabolism, 7- and 8-hydroxyefavirenz were incubated with a panel of expressed CYP enzymes. As the MS/MS characteristics of the dihydroxylated metabolite were the same as those of 8,14-dihydroxyefavirenz, quantification of the dihydroxyefavirenz was made using standard curves of 8,14-dihydroxyefavirenz. CYP2B6 catalyzed formation of dihydroxyefavirenz from 7- and 8-hydroxyefavirenz at the highest rate compared to other CYPs (Figure 7A). Kinetics for the metabolism of 8-hydroxyefavirenz in expressed CYP2B6 (Figure 7B) was characterized by substrate inhibition kinetic model (V_{max} , 4.21 pmol/min/pmol P450; K_m , 23.2 μ M; and K_s , 23.4 μ M), while that of 7-hydroxyefavirenz was best described by Michaelis-Menten equation (V_{max} of 1.3 pmol/min/pmol P450 and a K_m of 62.4 μ M). At lower

substrate concentrations, 8-hydroxyefavirenz was more efficiently oxidized by CYP2B6 than 7-hydroxyefavirenz.

As described above, 8,14-dihydroxyefavirenz was not detected *in vitro* when efavirenz and 8-hydroxyefavirenz were used as substrates. However, this metabolite was detected and quantified in plasma samples obtained from subjects taking a single 600 mg oral dose of efavirenz (see below). *In vivo*, 8-hydroxyefavirenz is rapidly conjugated (glucuronidated or sulfated) (Mutlib, et al., 1999b). The possibility that 8-hydroxyefavirenz glucuronide might undergo 14-hydroxylation was tested by incubating 8-hydroxyefavirenz glucuronide with HLM samples and cofactors. A unique peak was noted (this was not observed in negative control experiments) at a retention time of 8.6 min in this incubation (data not shown). This peak was consistent with involvement of CYP-mediated reaction. In a panel of expressed CYPs, 8-hydroxyefavirenz glucuronide was converted to a metabolite peak mainly by expressed CYP2A6 (2.29 pmol/min/pmol P450) and to some extent by CYP1A2 (1.19 pmol/min/pmol P450) > CYP2B6 (0.21 pmol/min/pmol P450) (Supplemental Fig. 2). This metabolite is likely to be 14-hydroxylated of 8-hydroxyefavirenz glucuronide. However, attempts to confirm this suggestion through treatment of the microsomal incubates with β -glucuronidase and assay the metabolite hydrolyzed did not provide useful information, probably due to the fact that its formation *in vitro* was low.

C. Identification and quantification of efavirenz metabolites in vivo:

Efavirenz and its metabolites were analyzed in plasma samples obtained from healthy volunteers administered a single 600 mg oral dose of efavirenz. In Figure 8, MRM trace chromatograms of extracted blank plasma samples (Figure 8A) and of extracted plasma samples 3 hours after efavirenz dosing (Figure 8B) are shown. All the primary (7- and 8-

hydroxyefavirenz) and secondary (dihydroxylated efavirenz) metabolites that were characterized *in vitro* were detected in the clinical samples (Figure 8B). Efavirenz and metabolites were not detected in (blank) plasma samples obtained from same subjects before efavirenz administration (data not shown). A metabolite that had the same retention time and MS/MS characteristics to those of synthetic standard 8,14-dihydroxyefavirenz was identified *in vivo* (Figure 8). This metabolite was not formed (detected) *in vitro* from any of the substrates tested (efavirenz, 7- or 8-hydroxyefavirenz).

The concentrations versus time curves of efavirenz and its metabolites in healthy volunteers (n=5) administered a single 600 mg oral dose of efavirenz are shown in Figure 9A. The pharmacokinetic data provided are total concentrations (free + conjugated) of efavirenz and its metabolites quantified after incubation of the samples with β -glucuronidase (“deconjugation”). The β -glucuronidase that was used also contained sulfatase and thus could not reliably distinguish between glucuronide and sulfate conjugates. Although it is likely that these conjugates are mostly glucuronides (Mutlib, et al., 1999b), conjugates are used in this manuscript to reflect nonselectivity of the enzymatic hydrolysis used. The plasma area under the plasma concentrations time curves (AUC_{0-72}) of efavirenz and metabolites are provided in Figure 9B. Based on the AUC_{0-72} in plasma, efavirenz was the most abundant followed by 8-hydroxyefavirenz > 7-hydroxyefavirenz > 8,14-dihydroxyefavirenz > dihydroxylated efavirenz.

DISCUSSION:

The major new findings of the present study were the demonstration that: CYP2A6-mediated efavirenz 7-hydroxylation accounts for ~23% of efavirenz metabolism; CYP2A6 is a partial contributor towards efavirenz 8-hydroxylation; efavirenz is metabolized sequentially to novel dihydroxylated metabolite(s), via CYP2B6-mediated 7- and 8-hydroxyefavirenz hydroxylation as intermediary; and 8,14-dihydroxyefavirenz is formed *in vivo* but not *in vitro*, suggesting novel metabolic reactions and challenging previous notion that it is formed through direct 14-hydroxylation of 8-hydroxyefavirenz (Mutlib, et al., 1999b; Ward, et al., 2003). The identification and quantification of all efavirenz primary (7- and 8-hydroxyefavirenz) and secondary (8,14-dihydroxyefavirenz and a dihydroxylated) metabolites and the first demonstration of their full pharmacokinetics in plasma of healthy subject taking a single 600 mg oral dose of efavirenz confirm clinical relevance of the *in vitro* findings. Finally, the role CYP2B6 plays in efavirenz 8-hydroxylation, a metabolic route accounting for ~77% of efavirenz clearance, was further confirmed (Ward, et al., 2003). These data should help to predict determinants of efavirenz metabolism and response. They should also form the scientific basis with which to select the most appropriate pharmacokinetic parameters when efavirenz is used to assess the activity of CYP2B6 (and possibly CYP2A6) *in vivo*.

The *in vitro* data reported here show that 7- and 8-hydroxyefavirenz are the primary metabolites of efavirenz and concur with previous reports (Mutlib, et al., 1999b; Ward, et al., 2003; Desta, et al., 2007). On the basis of the *in vitro* CL_{int} in HLM samples, 7- and 8-hydroxylation on the average account for ~22.5% and ~77.5% of efavirenz overall metabolism (Table 1). Provided the contribution of other elimination routes [e.g. efavirenz N-glucuronidation

(Belanger, et al., 2009); and nonhepatic clearance (Mutlib, et al., 1999b)] are minimal, 7- and 8-hydroxylation represent minor and major clearance mechanisms of efavirenz.

The identification of new and novel dihydroxylated efavirenz in microsomal incubates of efavirenz, 7- and 8-hydroxyefavirenz suggests that efavirenz is sequentially oxidized, with monohydroxylated efavirenz as intermediary. Efavirenz secondary metabolism via 8-hydroxyefavirenz to 8,14-dihydroxyefavirenz has been previously proposed *in vitro* (Ward, et al., 2003) and *in vivo* (Mutlib, et al., 1999b). However, 14-hydroxylation of 8-hydroxyefavirenz was not observed in the present *in vitro* study as the dihydroxylated metabolite(s) formed was not consistent with 8,14-dihydroxyefavirenz. In addition, efavirenz secondary metabolism can undergo via 7-hydroxyefavirenz to dihydroxylated efavirenz. The precise structural identity of the dihydroxylated metabolite(s) remains unknown. It is possible that the secondary hydroxylation site may occur at C-15 or C-16 portion of the cyclopropyl part of the molecule, resulting in MS/MS properties indistinguishable with those of 8,14-dihydroxyefavirenz. It is also unclear whether the metabolite formed from 7-hydroxyefavirenz is the same as that formed from 8-hydroxyefavirenz. As attempts to separate the metabolites formed from 7- and 8-hydroxyefavirenz chromatographically did not yield useful information, the metabolites formed may have similar physico-chemical characteristics. Theoretically, 7- and 8-hydroxyefavirenz can undergo 8-hydroxylation and 7-hydroxyefavirenz, respectively, resulting in the formation of 7,8-dihydroxyefavirenz. This possibility cannot be ruled out but may be questionable by the fact that the most abundant MS/MS fragments of the dihydroxylated metabolite were similar to those from 8,14-dihydroxyefavirenz.

The *in vivo* relevance of the *in vitro* findings is shown by the fact that all the primary and secondary metabolites of efavirenz that were identified *in vitro* were confirmed in plasma

samples of healthy volunteers after deconjugation. These data represent the first comprehensive description of efavirenz metabolite pharmacokinetics and mirrors the relative differences in the *in vitro* intrinsic clearances of 7- and 8-hydroxyefavirenz, providing support to the *in vivo* relevance of the *in vitro* findings. Interestingly, 8,14-dihydroxyefavirenz, a metabolite that was not detected *in vitro*, was positively identified and quantified in the clinical samples treated with β -glucuronidase. The reason for the lack of *in vitro* and *in vivo* correlation is not clear. *In vivo*, 8-hydroxyefavirenz is rapidly conjugated (glucuronidated and/or sulfated) by phase II enzymes (Mutlib et al., 1999b). It is possible that the conjugated 8-hydroxyefavirenz undergoes 14-hydroxylation *in vivo*, from which 8,14-dihydroxyefavirenz could be released upon treatment of efavirenz plasma samples with β -glucuronidase as observed in our study. Consistent with this suggestion, Mutlib et al., reported a glucuronide (C14)-sulfate (C8) diconjugate of dihydroxylated efavirenz in urine and bile of rats administered efavirenz, 8-hydroxyefavirenz or 8-hydroxyefavirenz sulfate (Mutlib, et al., 1999a). Other examples show that sulfate or glucuronide metabolites can undergo oxidation by CYPs [(Mutlib, et al., 1999a; Delaforge, et al., 2005) and references therein]. Preliminary proof of concept in support of oxidation of a conjugated 8-hydroxyefavirenz was obtained in the present study where a metabolite peak that was consistent with involvement of CYPs (CYP2A6, CYP1A2 and CYP2B6) was noted when 8-hydroxyefavirenz glucuronide was incubated with HLM samples and cofactors. Together, these data begin to provide a mechanistic understanding by revealing novel metabolic reactions of efavirenz.

Comprehensive set of *in vitro* experiments were conducted to identify the CYPs involved in efavirenz primary and secondary metabolism. Formation rate of 7-hydroxyefavirenz was: substantially inhibited by selective CYP2A6 inhibitors pilocarpine (Bourrie, et al., 1996) and

letrozole CYP2A6 inhibitor (Jeong, et al., 2009b) (Figure 5); correlated significantly with CYP2A6 activity (Table 2); and catalyzed exclusively by expressed CYP2A6 (Figure 4). The K_m values derived from HLM samples and expressed CYP2A6 (Table 1) were very close suggesting that the enzyme catalyzing 7-hydroxylation of efavirenz in HLM samples is CYP2A6. Efavirenz 7-hydroxylation in HLM samples was inhibited by thioTEPA (Table 3). It is likely that this is mediated by the ability of thioTEPA to inhibit CYP2A6 rather than involvement of CYP2B6 in this reaction because expressed CYP2B6 was not found to be capable of efavirenz 7- hydroxylation (see below). ThioTEPA potently inhibits CYP2B6 (Rae, et al., 2002; Ward, et al., 2003; Harleton, et al., 2004; Richter, et al., 2005), but its selectivity has been questioned recently by other authors (Turpeinen, et al., 2004; Obach, et al., 2006; Walsky and Obach, 2007). The present data provide additional support that thioTEPA may inhibit CYP2A6 in addition to CYP2B6.

The kinetic, inhibition and correlation analyses in HLM samples and data from expressed CYPs confirm previous findings that CYP2B6 is the principal catalyst of efavirenz 8-hydroxylation (Ward, et al., 2003; Desta, et al., 2007). However, these data also implicate for the time that CYP2A6 in catalyzing efavirenz 8-hydroxylation. First, pilocarpine inhibited efavirenz 8-hydroxylation in HLMs and expressed CYP2B6. Clearly, pilocarpine is frequently used as selective inhibitor of CYP2A6 *in vitro*, but its selectivity has been poorly validated. Its ability to inhibited CYP2B6-catalyzed reaction (present data) and previous report showing its inhibitory effect on CYP2C9 (Bourrie, et al., 1996) suggest that pilocarpine may not be highly selective towards CYP2A6. However, all the effects of pilocarpine on efavirenz 8-hydroxylation might not be explained by nonselectivity alone. The involvement of CYP2A6 in efavirenz 8-hydroxylation is supported by the fact that: pilocarpine inhibited 8-hydroxylation of efavirenz more in HLM

samples than in expressed CYP2B6 (Table 3); letrozole modestly inhibited efavirenz 8-hydroxylation (by 27%) (Figure 5); expressed CYP2A6 catalyzes efavirenz 8-hydroxylation (Figure 4); and CYP2A6 activity is significantly correlated with formation rate of 8-hydroxyefavirenz (Table 2). Therefore, CYP2A6 appears to contribute to the overall clearance of efavirenz by being the sole catalyst of efavirenz 7-hydroxylation, a pathway that accounts on the average for ~23% of efavirenz metabolism with large interindividual variability, and by participating (~20-30%) in efavirenz 8-hydroxylation.

Efavirenz has been recently described as a preferred marker of CYP2B6 activity *in vitro* and *in vivo* (Ward, et al., 2003; US Food and Drug Administration, 2006). The present data also support that it may serve as CYP2A6 probe. While the primary and secondary metabolites of efavirenz are pharmacologically inactive, identifying CYPs that catalyze them is important to select the most appropriate metabolic ratios that best describes CYP2B6 and CYP2A6 activities *in vivo*. That CYP2B6 was found to be the primary catalyst of 7- and 8-hydroxyefavirenz to the respective dihydroxylated metabolite (Figure 7B) provides important information in this respect. Moreover, the data show that monohydroxylated efavirenz metabolites, as with efavirenz, are efficient substrates of CYP2B6 irrespective of the site of hydroxylation. This information may help to model and better understand the active site of CYP2B6.

The findings presented here may have important implications. First, they suggest that CYP2B6 and CYP2A6 activity may influence efavirenz exposure and response. That CYP2B6 metabolic status is key determinant of efavirenz exposure and probably response in HIV patients has been established [e.g. (Tsuchiya, et al., 2004; Haas, et al., 2004; Rotger, et al., 2007; Zanger, et al., 2007)]. CYP2A6 activity exhibits large interindividual variation (Pelkonen, et al., 2000; Di, et al., 2009), mostly due to *CYP2A6* gene polymorphisms, but also as a result of exposure to

inducers and inhibitors of the enzyme (Nakajima, et al., 2006; Mwenifumbo and Tyndale, 2009; Di, et al., 2009). Recently, CYP2A6 genetic variation has been shown to influence efavirenz exposure in HIV patients (di Iulio, et al., 2009; Arab-Alameddine, et al., 2009; Kwara, et al., 2009a, 2009b). Second, efavirenz may serve as an effective probe of CYP2B6 and CYP2A6 activity *in vitro* and *in vivo*. The identification of novel metabolic pathways and CYPs involved in efavirenz primary and secondary metabolism should facilitate identification of efavirenz pharmacokinetic parameters that best reflect CYP2B6 and CYP2A6 activities *in vivo*. Clinical studies are ongoing to clarify the precise contribution of CYP2A6 and CYP2B6 in efavirenz metabolism using genetics and drug interactions as markers.

Acknowledgements

The project described was supported by Award Number R01GM078501 and R56 grant (2R56GM067308-09A1) from the National Institute of General Medical Sciences, National Institutes of Health (Bethesda, MD).

Disclaimer

The content is solely the responsibility of the authors and does not necessarily represent the official views of the National Institute of General Medical Sciences or the National Institutes of Health.

REFERENCES

- Arab-Alameddine M, di IJ, Buclin T, Rotger M, Lubomirov R, Cavassini M, Fayet A, Decosterd L, Eap C, Biollaz J, Telenti A and Csajka C (2009) Pharmacogenetics-Based Population Pharmacokinetic Analysis of Efavirenz in HIV-1-Infected Individuals. *Clin Pharmacol Ther* **85**:485-494.
- Belanger AS, Caron P, Harvey M, Zimmerman PA, Mehlotra RK and Guillemette C (2009) Glucuronidation of the antiretroviral drug efavirenz (EFV) by UGT2B7 and an in vitro investigation of drug-drug interaction with zidovudine (AZT). *Drug Metab Dispos* **37**:1793-1796.
- Bourrie M, Meunier V, Berger Y and Fabre G (1996) Cytochrome P450 isoform inhibitors as a tool for the investigation of metabolic reactions catalyzed by human liver microsomes. *J Pharmacol Exp Ther* **277**:321-332.
- Bristol-Myers Squibb Company, Package insert of efavirenz (Sustiva) (2009) at http://packageinserts.bms.com/pi/pi_sustiva.pdf (Updated September 2009).
- Csajka C, Marzolini C, Fattinger K, Decosterd LA, Fellay J, Telenti A, Biollaz J and Buclin T (2003) Population pharmacokinetics and effects of efavirenz in patients with human immunodeficiency virus infection. *Clin Pharmacol Ther* **73**:20-30.
- Delaforge M, Pruvost A, Perrin L and Andre F (2005) Cytochrome P450-mediated oxidation of glucuronide derivatives: example of estradiol-17beta-glucuronide oxidation to 2-hydroxy-estradiol-17beta-glucuronide by CYP 2C8. *Drug Metab Dispos* **33**:466-473.

Desta Z, Saussele T, Ward B, Blievernicht J, Li L, Klein K, Flockhart DA and Zanger UM (2007) Impact of CYP2B6 polymorphism on hepatic efavirenz metabolism in vitro. *Pharmacogenomics* **8**:547-558.

di Iulio J, Fayet A, Rab-Alameddine M, Rotger M, Lubomirov R, Cavassini M, Furrer H, Gunthard HF, Colombo S, Csajka C, Eap CB, Decosterd LA and Telenti A (2009) In vivo analysis of efavirenz metabolism in individuals with impaired CYP2A6 function. *Pharmacogenet Genomics* **19**:300-309.

Di YM, Chow VD, Yang LP and Zhou SF (2009) Structure, Function, Regulation and Polymorphism of Human Cytochrome P450 2A6. *Curr Drug Metab.* Sep 1. [Epub ahead of print]

Ekins S and Wrighton SA (1999) The role of CYP2B6 in human xenobiotic metabolism. *Drug Metab Rev* **31**:719-754.

U.S. Food and Drug Administration (2006) Draft Guidance for Industry: Drug Interaction Studies — Study Design, Data Analysis and Implications for Dosing and Labeling.

Haas DW, Ribaldo HJ, Kim RB, Tierney C, Wilkinson GR, Gulick RM, Clifford DB, Hulgath T, Marzolini C and Acosta EP (2004) Pharmacogenetics of efavirenz and central nervous system side effects: an Adult AIDS Clinical Trials Group study. *AIDS* **18**:2391-2400.

Harleton E, Webster M, Bumpus NN, Kent UM, Rae JM and Hollenberg PF (2004) Metabolism of N,N',N''-triethylenethiophosphoramidate by CYP2B1 and CYP2B6 results in the inactivation of both isoforms by two distinct mechanisms. *J Pharmacol Exp Ther* **310**:1011-1019.

Hodgson E and Rose RL (2007) The importance of cytochrome P450 2B6 in the human metabolism of environmental chemicals. *Pharmacol Ther* **113**:420-428.

Jeong S, Nguyen PD and Desta Z (2009a) Comprehensive in vitro inhibition analysis of 8 cytochrome P450 (CYP) enzymes by voriconazole: major effect on CYPs 2B6, 2C9, 2C19 and 3A. *Antimicrob Agents Chemother* **53**:541-551..

Jeong S, Woo MM, Flockhart DA and Desta Z (2009b) Inhibition of drug metabolizing cytochrome P450s by the aromatase inhibitor drug letrozole and its major oxidative metabolite 4,4'-methanol-bisbenzotrile in vitro. *Cancer Chemother Pharmacol* **64**:867-875.

Kwara A, Lartey M, Sagoe KW, Kenu E and Court MH (2009a) CYP2B6, CYP2A6 and UGT2B7 genetic polymorphisms are predictors of efavirenz mid-dose concentration in HIV-infected patients. *AIDS* **23**:2101-2106.

Kharasch ED, Mitchell D, Coles R (2008) Stereoselective bupropion hydroxylation as an in vivo phenotypic probe for cytochrome P4502B6 (CYP2B6) activity. *J Clin Pharmacol* **48**:464-474.

Kwara A, Lartey M, Sagoe KW, Rzek NL and Court MH (2009b) CYP2B6 (c.516G-->T) and CYP2A6 (*9B and/or *17) polymorphisms are independent predictors of efavirenz plasma concentrations in HIV-infected patients. *Br J Clin Pharmacol* **67**:427-436.

Marzolini C, Telenti A, Decosterd LA, Greub G, Biollaz J and Buclin T (2001) Efavirenz plasma levels can predict treatment failure and central nervous system side effects in HIV-1-infected patients. *AIDS* **15**:71-75.

Mo SL, Liu YH, Duan W, Wei MQ, Kanwar JR and Zhou SF (2009) Substrate Specificity, Regulation, and Polymorphism of Human Cytochrome P450 2B6. *Curr Drug Metab Sep* 1. [Epub ahead of print]

- .Mouly S, Lown KS, Kornhauser D, Joseph JL, Fiske WD, Benedek IH and Watkins PB (2002) Hepatic but not intestinal CYP3A4 displays dose-dependent induction by efavirenz in humans. *Clin Pharmacol Ther* **72**:1-9.
- Mutlib AE, Chen H, Nemeth G, Gan LS and Christ DD (1999a) Liquid chromatography/mass spectrometry and high-field nuclear magnetic resonance characterization of novel mixed diconjugates of the non- nucleoside human immunodeficiency virus-1 reverse transcriptase inhibitor, efavirenz. *Drug Metab Dispos* **27**:1045-1056.
- Mutlib AE, Chen H, Nemeth GA, Markwalder JA, Seitz SP, Gan LS and Christ DD (1999b) Identification and characterization of efavirenz metabolites by liquid chromatography/mass spectrometry and high field NMR: species differences in the metabolism of efavirenz. *Drug Metab Dispos* **27**:1319-1333.
- Mwenifumbo JC and Tyndale RF (2009) Molecular genetics of nicotine metabolism. *Handb Exp Pharmacol* 235-259.
- Nakajima M, Fukami T, Yamanaka H, Higashi E, Sakai H, Yoshida R, Kwon JT, McLeod HL and Yokoi T (2006) Comprehensive evaluation of variability in nicotine metabolism and CYP2A6 polymorphic alleles in four ethnic populations. *Clin Pharmacol Ther* **80**:282-297.
- Newton DJ, Wang RW and Lu AY (1995) Cytochrome P450 inhibitors. Evaluation of specificities in the in vitrometabolism of therapeutic agents by human liver microsomes. *Drug Metab Dispos* **23**:154-158.
- Obach RS, Walsky RL and Venkatakrisnan K (2006) Mechanism-based inactivation of human cytochrome P450 enzymes and the prediction of drug-drug interactions. *Drug Metab Dispos* **35**:246-255

Pelkonen O, Rautio A, Raunio H and Pasanen M (2000) CYP2A6: a human coumarin 7-hydroxylase. *Toxicology* **144**:139-147.

Rae JM, Soukhova NV, Flockhart DA and Desta Z (2002) Triethylenethiophosphoramidate is a specific inhibitor of cytochrome P450 2B6: implications for cyclophosphamide metabolism. *Drug Metab Dispos* **30**:525-530.

Richter T, Murdter TE, Heinkele G, Pleiss J, Tatzel S, Schwab M, Eichelbaum M and Zanger UM (2004) Potent mechanism-based inhibition of human CYP2B6 by clopidogrel and ticlopidine. *J Pharmacol Exp Ther* **308**:189-197.

Richter T, Schwab M, Eichelbaum M and Zanger UM (2005) Inhibition of human CYP2B6 by N,N',N''-triethylenethiophosphoramidate is irreversible and mechanism-based. *Biochem Pharmacol* **69**:517-524.

Rotger M, Tegude H, Colombo S, Cavassini M, Furrer H, Decosterd L, Blievernicht J, Saussele T, Gunthard HF, Schwab M, Eichelbaum M, Telenti A and Zanger UM (2007) Predictive value of known and novel alleles of CYP2B6 for efavirenz plasma concentrations in HIV-infected individuals. *Clin Pharmacol Ther* **81**:557-566.

Tsuchiya K, Gatanaga H, Tachikawa N, Teruya K, Kikuchi Y, Yoshino M, Kuwahara T, Shirasaka T, Kimura S and Oka S (2004) Homozygous CYP2B6 *6 (Q172H and K262R) correlates with high plasma efavirenz concentrations in HIV-1 patients treated with standard efavirenz-containing regimens. *Biochem Biophys Res Commun* **319**:1322-1326.

Turpeinen M, Nieminen R, Juntunen T, Taavitsainen P, Raunio H and Pelkonen O (2004) Selective inhibition of CYP2B6-catalyzed bupropion hydroxylation in human liver microsomes in vitro. *Drug Metab Dispos* **32**:626-631.

Walsky RL and Obach RS (2007) A comparison of 2-phenyl-(1-piperidinyl)propane (PPP), ThioTEPA, clopidogrel and ticlopidine as selective inactivators of human cytochrome P4502B6.

Drug Metab Dispos **35**:2053-2059

Wang H and Tompkins LM (2008) CYP2B6: new insights into a historically overlooked cytochrome P450 isozyme. *Curr Drug Metab* **9**:598-610.

Ward BA, Gorski JC, Jones DR, Hall SD, Flockhart DA and Desta Z (2003) The cytochrome P4502B6 (CYP2B6) is the main catalyst of efavirenz primary and secondary metabolism: Implication for HIV/AIDS therapy and utility of efavirenz as a substrate marker of CYP2B6 catalytic activity. *J Pharmacol Exp Ther* **306**:287-300.

Zanger UM, Klein K, Saussele T, Bliedernicht J, Hofmann H and Schwab M (2007) Polymorphic CYP2B6: molecular mechanisms and emerging clinical significance. *Pharmacogenomics* **8**:743-759.

Footnotes:

The work was supported by the National Institute of Health National Institute of General Medical Sciences [Grants: R01GM078501, 2R56GM067308-09A1], Bethesda, MD, USA.

Disclaimer: The content is solely the responsibility of the authors and does not necessarily represent the official views of the National Institute of General Medical Sciences or the National Institutes of Health.

Reprint requests to:

Dr. Zeruesenay Desta

Department of Medicine/Division of Clinical Pharmacology

Indiana University School of Medicine

1001 West 10th Street, WD Myers Bldg., W7123 Indianapolis, IN 46202, USA

E-mail: zdesta@iupui.edu

Legend to Figures

Figure 1. Multiple reaction monitoring (MRM) trace chromatograms of efavirenz (EFV) in human liver microsomal incubates. Efavirenz (20 μ M) was incubated with HLM samples and cofactors. Subsequent sample processing and LC/MS/MS conditions were as described in the *Methods* section. Metabolites that were consistent with monohydroxylated (7- and 8-hydroxyEFV) and secondary metabolite (dihydroxylated EFV) were identified in the microsomal incubates. Nevirapine was used as an internal standard.

Figure 2. Representative kinetics for the metabolism of efavirenz (EFV) to 7-hydroxyEFV and 8-hydroxyEFV in human liver samples (IU42). Increasing concentrations of EFV (5–150 μ M) was incubated with HLM samples (0.25 mg/ml) and cofactors for 10 min at 37°C. Formation rates of metabolites (pmol/min/mg protein) versus EFV concentration (μ M) were best fit to a one site hyperbolic Michaelis-Menten equation (**A**) (see *Data Analysis*). The corresponding Eadie-Hofstee plots are shown (**B**). Each point represents the average of duplicate incubations. Kinetic parameters derived from these and other six HLM samples are listed in Table 1.

Figure 3. Efavirenz (EFV) metabolism in a panel of 15 characterized HLMs. EFV (10 μ M) was incubated with microsomes from different human livers (0.25 mg/ml) and cofactors for 15 min at 37°C. Formation rates (pmol of product/min/mg protein) of 7-hydroxyEFV (7-OHEFV) (**A**) and of 8-hydroxyEFV (8-OHEFV) (**B**) are shown. Rates represent average of duplicate incubation measurements. Correlations between formation rates of 7-OHEFV or 8-OHEFV and the activity of CYP enzymes are illustrated in Table 2.

Figure 4. Efavirenz (EFV) metabolism by a panel of CYP enzymes. EFV (10 μ M or 100 μ M) was incubated with expressed CYPs (13 or 26 pmol P450) and cofactors for 10 min at 37°C. Rates (pmol of product/min/pmol of P450) of 7-hydroxyEFV (7-OHEFV) (**A**) and 8-hydroxyEFV (8-OHEFV) (**B**) are presented. Each point is an average of duplicate incubation measurements.

Figure 5. Inhibition of efavirenz (EFV) metabolism in HLM samples. EFV (10 μ M) was incubated with HLMs (0.25 mg/ml) and cofactors for 10 min at 37°C in the absence (control) and presences of CYP isoform specific inhibitor (See *Methods Section* for details). Data (% activity remaining after inhibition relative to the vehicle control) represent mean \pm SD of three duplicate measurements or 3 different HLMs. Abbreviations: ticlopidine (TICL), quercetin (QUER), troleandomycin (TAO), ketoconazole (KETO), pilocarpine (PILO), diethyldithiocarbamate (DEDTC), sulfaphenazole (SULF), furafylline (FURAF), letrozole (LTR) and quinidine (QUIN). The final concentrations of these inhibitors used are indicated in bracket. A preincubation protocol was used for FURAF, TAO, thioTEPA and DEDTC (see *Methods* section).

Figure 6: Multiple reaction monitoring (MRM) trace chromatograms of 7-hydroxyefavirenz (7-OHEFV) and 8-hydroxyefavirenz (8-OHEFV) in human liver microsomal incubates. Each substrate (5 μ M) was incubated in HLM samples and cofactors for 10 min at 37°C. A metabolite peak that was consistent with dihydroxylated efavirenz was formed in microsomal incubations of 7-OHEFV (**A**) and 8-OHEFV (**B**). Synthetic 8,14-dihydroxyefavirenz (8,14-diOHEFV) standard was directly injected (**C**).

Figure 7. Secondary metabolism of efavirenz (EFV) by a panel of expressed CYPs. Sequential metabolism was tested using 7-hydroxyEFV (7-OHEFV) and 8-hydroxyEFV (8-

OHEFV) as substrates. 7-OHEFV (5 μ M) and 8-OHEFV (5 μ M) were incubated with expressed CYPs (13 or 26 pmol P450) and cofactors for 10 min at 37°C and the formation of a dihydroxylated efavirenz was monitored (**A**). Kinetics for the metabolism of 7-OHEFV and 8-OHEFV to dihydroxylated efavirenz was determined by incubating each substrate (1 μ M to 150 μ M) with 13 pmol CYP2B6 and cofactors for 10 min at 37°C (**B**). Kinetic analysis was performed by fitting to a one site hyperbolic Michaelis Menten equation (7-OHEFV metabolism) or using substrate inhibition equation (8-OHEFV) (see *Data Analysis*). Each point represents average pmol of product/min/pmol of CYP2B6 of duplicate incubation measurements.

Figure 8. Representative MRM trace chromatograms of efavirenz (EFV) and its monohydroxylated (7- and 8-hydroxyefavirenz) and secondary metabolites (8,14-dihydroxyefavirenz and dihydroxyefavirenz) in plasma samples obtained from subjects administered a single 600 mg oral dose of efavirenz. Extracted blank samples spiked with authentic standards of efavirenz and its metabolites (**A**); and extracted plasma sample obtained 3 hours after administration of a single 600 mg oral dose of efavirenz to healthy volunteers (**B**). Plasma samples were treated with β -glucuronidase and the peaks represent total (free + conjugated).

Figure 9. Pharmacokinetics of efavirenz (EFV) and its primary and secondary metabolites in healthy volunteer subjects (n=5) administered a single 600 mg oral dose of EFV. Plasma concentrations versus time curves (**A**) and area under the concentration-time curve (AUC_{0-72}) (**B**) of efavirenz and metabolites are shown. (8-OHEFV, 8-hydroxyEFV; 7-OHEFV, 7-hydroxyEFV; 8,14-diOHEFV, 8,14-dihydroxyefavirenz; diOHEFV, dihydroxylated EFV).

Table 1. Kinetic parameters for the formation of 8-hydroxyefavirenz and 7-hydroxyefavirenz from efavirenz in 7 different HLM samples and expressed CYP2A6 and CYP2B6.

HLMs	8-hydroxyefavirenz				7-hydroxyefavirenz			
	V_{max}	K_m	Cl_{int}	% of total	V_{max}	K_m	Cl_{int}	% of total
			(V_{max}/K_m)	Cl_{int}			(V_{max}/K_m)	Cl_{int}
IU6 84	.4	19.4	4.37	62.7	48.7	18.8	2.60	37.3
IU31 51	.8	7.6	6.86	83.4	10.7	7.8	1.37	16.6
IU42 17	.9	7.1	2.52	89.0	7.5	23.9	0.31	11.0
IU59 30	.9	7.9	3.90	79.0	8.6	8.3	1.04	21.0
IU58	28.7 25	.2	1.14	90.2	2.2	17.5	0.12	9.8
IU65 24	.8	12.4	2.00	61.5	16.8	13.4	1.25	38.5
HLT 13	9.6	9.5	14.75	77.1	57.0	13.0	4.38	22.9
Mean 54	.0	12.7	5.10	77.5	21.6	14.7	1.58	22.5
SD 43	.9	7.0	4.66	11.6	21.9	5.8	1.47	11.6
Expressed CYPs								
CYP2B6	1.4 9.	0	0.16					
CYP2A6	0.6 7.	7	0.08		0.4	7.6	0.05	

Abbreviations: V_{max} , pmol/min/mg protein or pmol/min/pmol P450; K_m , μ M; Cl_{int} , (μ l/min/mg protein or μ l/min/pmol P450).

Increasing concentrations of efavirenz (1-150 μ M) were incubated with HLM samples (0.25 mg/ml) and cofactors at 37°C (see Methods section). Kinetic parameters for the formation of 8-hydroxyefavirenz and 7-

hydroxyefavirenz were estimated by fitting the velocity vs. substrate concentrations to Michaelis-Menten equation as described in the Data Analysis section. Kinetic parameters in the individual HLM samples (standard errors of parameter estimates) are presented. In vitro intrinsic clearance (CL_{int}) was calculated. Percent contribution to the overall clearance was estimated as follows $CL_{int}(\text{metab}) \times 100 / CL_{int}(\text{total})$. $CL_{int}(\text{total})$ is the sum of CL_{int} of 7- and 8-hydroxyefavirenz. Assumptions: 1) these two pathways are the main clearance mechanisms; 2) efavirenz N-glucuronidation is minor; 3) under the incubation conditions, sequential metabolism is minimal.

Table 2: Correlation of formation rates of 8-hydroxyefavirenz and 7-hydroxyefavirenz from efavirenz (10 μ M) with the activities of different CYP enzymes in HLM samples (n=15).

CYP isoforms	Efavirenz metabolites			
	7-OHEFV 8		-OHEFV	
	Spearman r	P value	Spearman r	P value
CYP1A2 0.	31	0.26	0.53	0.044
CYP2A6	0.80 0	.0003	0.	62
CYP2B6 0.	57	0.03	0.81 0	.0003
CYP2C8	0.58 0.	02	0.58 0.	03
CYP2C9	0.30 0.	27	0.37 0.	17
CYP2C19	0.28 0.	32	0.03 0.	93
CYP2D6 -	0.20	0.48	0.08	0.79
CYP2E1	0.01 0.	98	0.22 0.	43
CYP3A (T)	0.61 0.	015	0.37	0.18
CYP4A11	0.25	0.36	0.004	0.99
FMO	0.21 0.	45	0.06 0.	84

Efavirenz (10 μ M) was incubated with microsomes from different human livers (0.25 mg/ml) and a NADPH-generating system for 15 min at 37°C. Data were analyzed using the nonparametric correlation test (Spearman *r*). The activity of each isoform was determined using the respective specific substrate probe reaction (see *Materials and Methods*). CYP3A was assayed using testosterone (T). $p < 0.05$ is considered statistically significant.

Table 3. Inhibition of efavirenz 7- and 8-hydroxylation by thioTEPA, pilocarpine and ticlopidine in HLM samples and expressed CYP2A6 and CYP2B6.

Inhibitor	Microsomes	7-hydroxylation		8-Hydroxylation	
		% activity remaining	IC ₅₀ (μM)	% activity remaining	IC ₅₀ (μM)
<u>ThioTEPA</u>					
	HLMs	55.0±1.4	31.7	32.3±4.3	9.8
	CYP2A6	17.4±0.6	6.6	17.5±1.4	6.9
	CYP2B6	--	--	44.9±0.2	-
<u>Pilocarpine</u>					
	HLMs	4.3±1.9	2.3	32.7±0.8	29.5
	CYP2A6	5.8±0.5	-	6.2±0.4	--
	CYP2B6	--	--	75.6±4.2	135.6
<u>Ticlopidine</u>					
	HLMs	150.8±11.1	-	18.1±0.6	--
	CYP2A6	77.5±6.4	-	77.8±6.2	--
	CYP2B6	--	--	27.0±0.5	-

Efavirenz (10 μM) was incubated for 10 min at 37°C in duplicate with HLM samples (0.25 mg/ml) (or 26 pmol CYP2A6 or 13 pmol CYP2B6) and cofactors in the absence (control) and presence of an inhibitor. For determination of % activity remaining, a single concentration of thioTEPA (50 μM), pilocarpine (50 μM) or ticlopidine (5 μM) was used. To determine the IC₅₀ values, multiple concentrations of thioTEPA (0-100 μM) or pilocarpine (0-100 μM) were used.

Figure 1

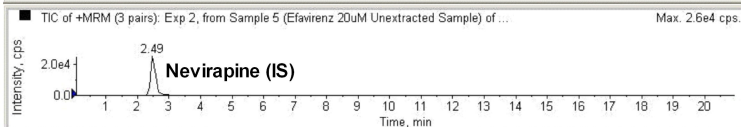
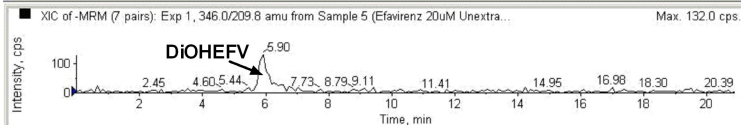
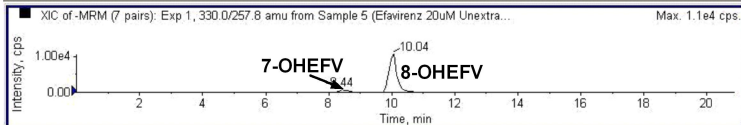
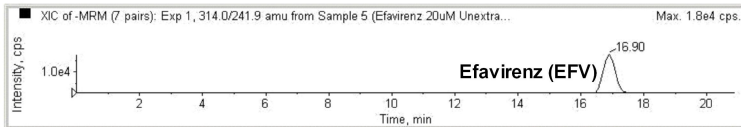


Figure 2

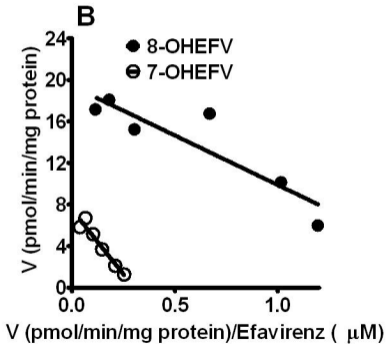
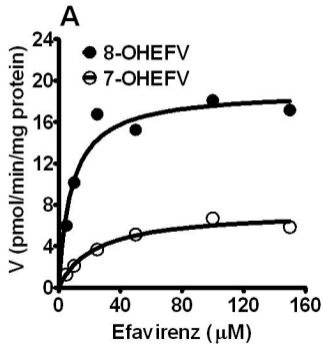


Figure 3

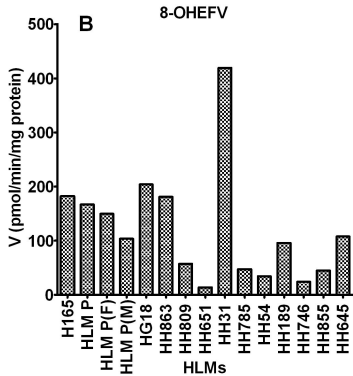
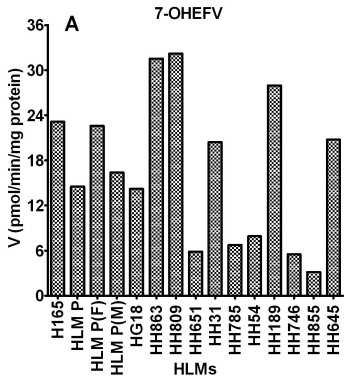


Figure 4

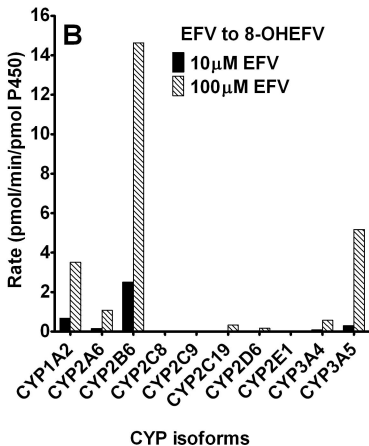
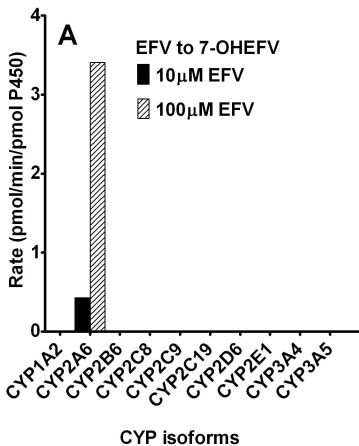
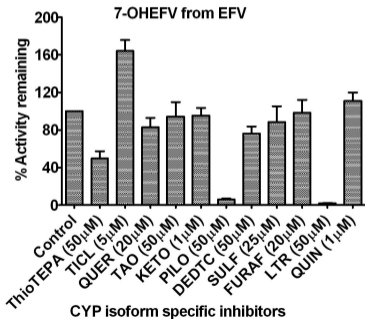


Figure 5

A



B

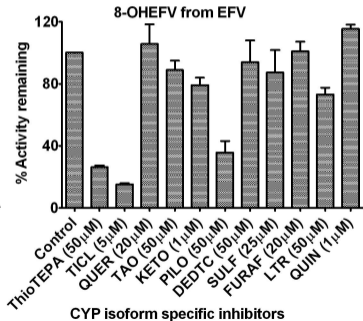
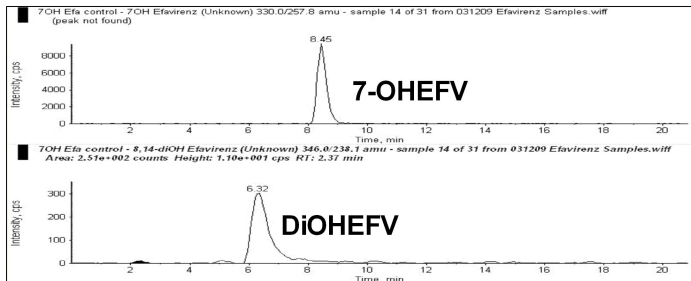
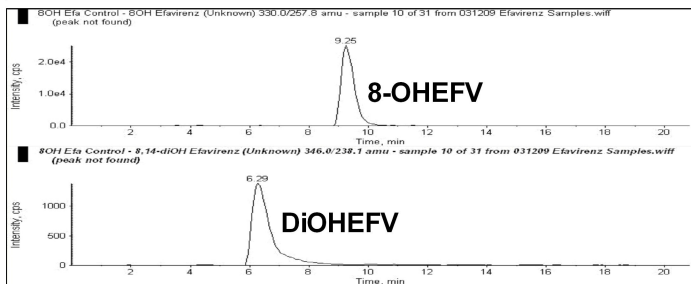


Figure 6

A



B



C

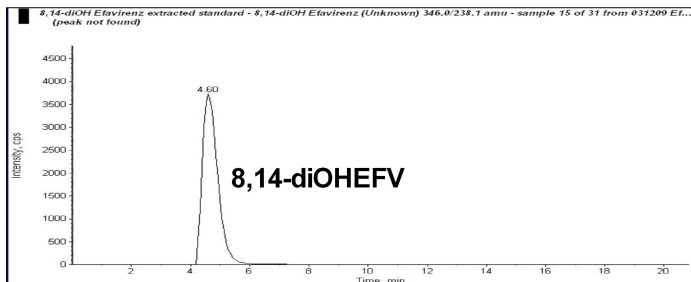


Figure 7

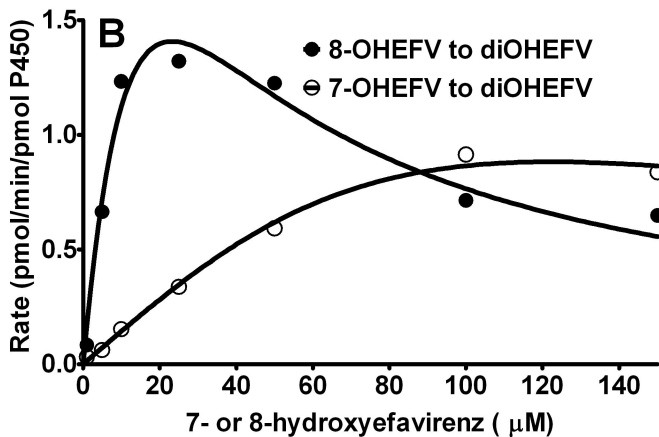
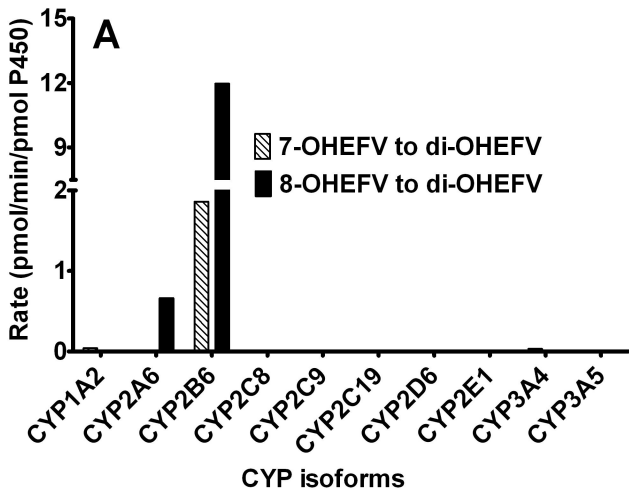
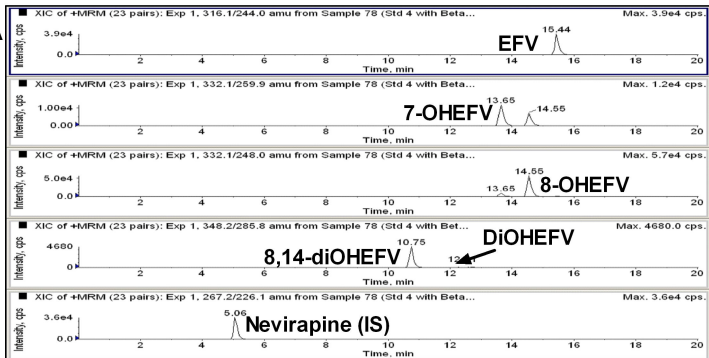


Figure 8

A



B

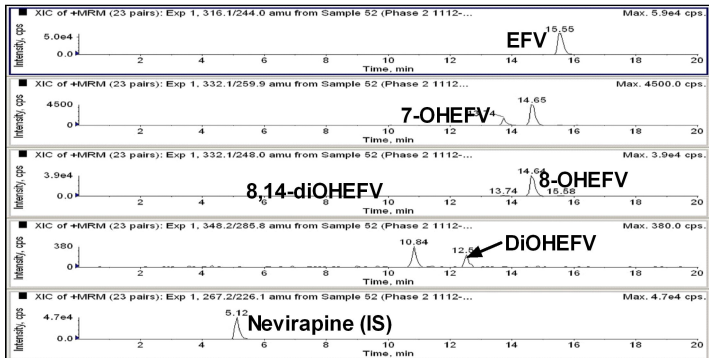
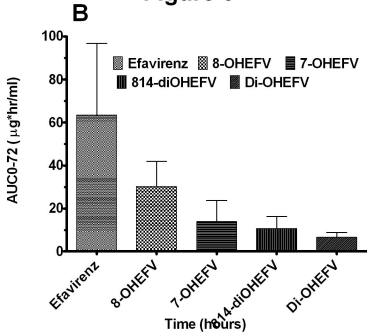
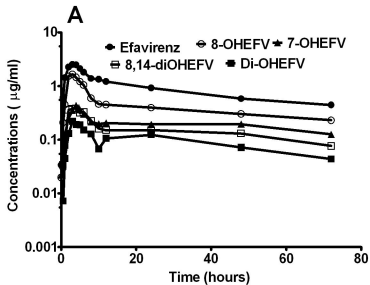


Figure 9

Title: Efavirenz primary and secondary metabolism *in vitro and in vivo*: identification of novel metabolic pathways and cytochrome P450 (CYP) 2A6 as the principal catalyst of efavirenz 7-hydroxylation.

Authors: Evan T. Ogburn, David R. Jones, Andrea R. Masters, Cong Xu, Yingying Guo, Zeruesenay Desta.

Journal: *Drug Metab Dispos*, 2010

Table 1. Mass spectrometry settings for efavirenz, 8-hydroxyefavirenz, 7-hydroxyefavirenz, 8,14-dihydroxyefavirenz and nevirapine using API2000.

Compound	Q1 (amu)	Q3 (amu)	Entrance Potential (V)	Collision Energy (V)	Cell Entrance Potential (V)	Exit Potential (V)
efavirenz	314.0	244, 242	-12	-18	-16	-22
8-hydroxyefavirenz	330.0	257.8, 210	-11	-20	-18	-24
7-hydroxyefavirenz	330.0	257.8, 210	-11	-20	-18	-24
8,14-dihydroxyefavirenz	346.0	274.3, 210, 238.1	-10	-30	-18.185	-15
nevirapine (positive mode)	267.2	226	4.5	30	14.1	15

Title: Efavirenz primary and secondary metabolism *in vitro* and *in vivo*: identification of novel metabolic pathways and cytochrome P450 (CYP) 2A6 as the principal catalyst of efavirenz 7-hydroxylation.

Authors: Evan T. Ogburn, David R. Jones, Andrea R. Masters, Cong Xu, Yingying Guo, Zeruesenay Desta.

Journal: *Drug Metab Dispos*, 2010

Table 2. Mass spectrometry settings for efavirenz, 8-hydroxyefavirenz, 7-hydroxyefavirenz, 8,14-dihydroxyefavirenz and nevirapine using API3200 in positive mode

Compound	Q1 (amu)	Q3 (amu)	Declustering Potential (V)	Entrance Potential (V)	Collision Energy (V)	Cell Entrance Potential (V)	Exit Potential (V)
efavirenz	316.0	244, 232	46	5.50	23	19.14	4
8-hydroxyefavirenz	332.12	248, 268	51	6	25	19.67	4
7-hydroxyefavirenz	332.12	260, 253	56	6	21	19.67	4
8,14-dihydroxyefavirenz	348.18	286, 266	26	6	17	20.20	4
nevirapine	267.2	226	61	4.5	35	17.53	4

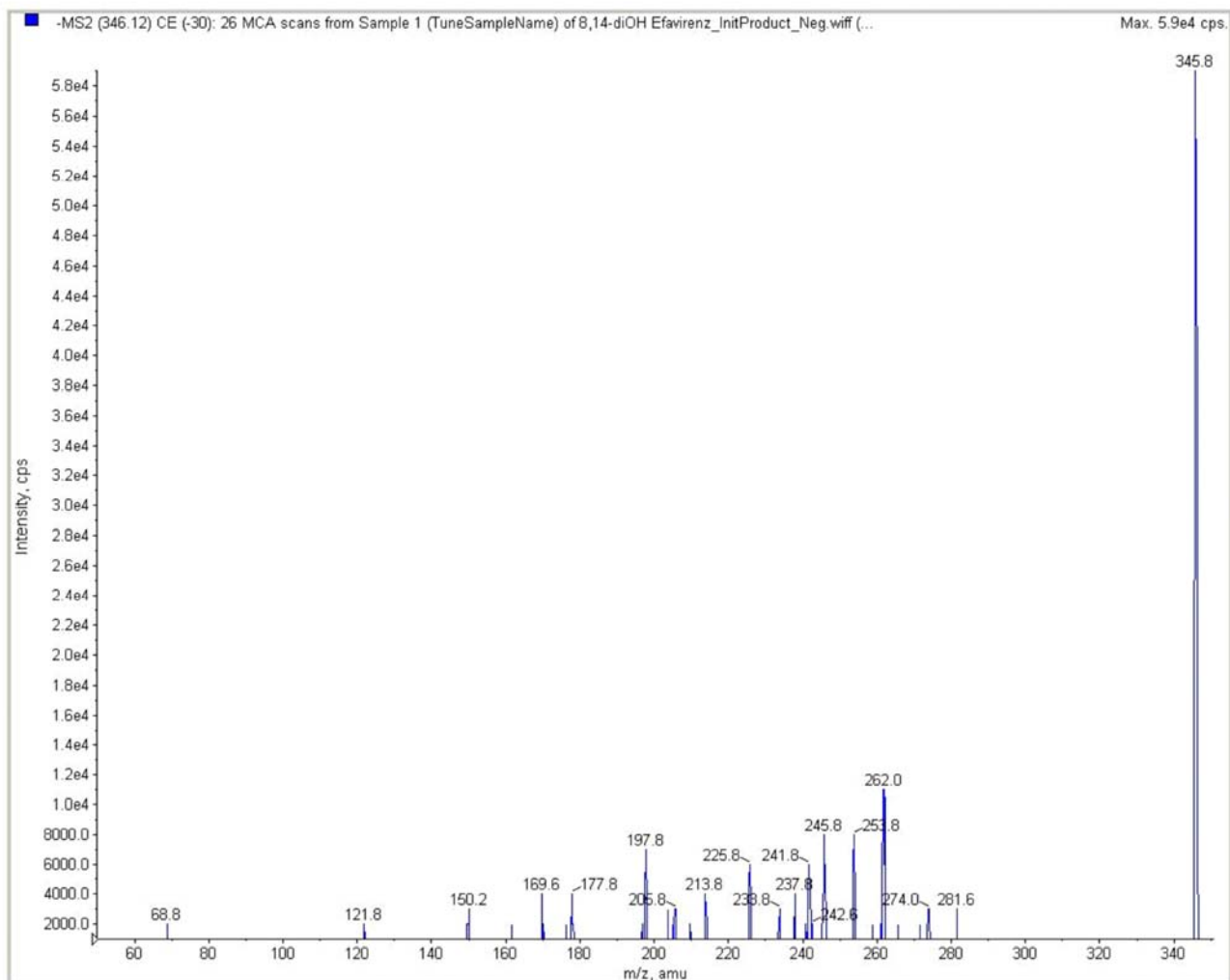
Title: Efavirenz primary and secondary metabolism *in vitro and in vivo*: identification of novel metabolic pathways and cytochrome P450 (CYP) 2A6 as the principal catalyst of efavirenz 7-hydroxylation.

Authors: Evan T. Ogburn, David R. Jones, Andrea R. Masters, Cong Xu, Yingying Guo, Zeruesenay Desta.

Journal: *Drug Metab Dispos*, 2010

Supplemental Figure 1. MS/MS product ion spectra after collision-induced dissociation of synthetic 8,14-dihydroxyefavirenz standard directly infused to the triple quadrupole mass spectrometer (**A**) and of a dihydroxylated metabolite from 8-hydroxyefavirenz (5 μ M) incubation in HLMs and cofactors (**B**) where, after the signal generated by the parent ion mass m/z 346, samples were reinjected in to LC/MS/MS and subject to product ion scan (Q3) range of m/z 100 to 400.

Supplemental Figure 1A



Supplemental Figure 1B

